European Journal of Molecular & Clinical Medicine
ISSN 2515-8260 Volume 07, Issue 03, 2020

An Efficient Segmentation Of Optic Disc Using Convolution Neural Network For Glaucoma Detection In Retinal Images

C. Raja[1], Dr. N. Vinodhkumar[2]

[1]*Associate Professor*
Department of ECE
Vignsn's Foundation for Science, Technology & Research
Andhra Pradesh, India
rajachandru82@yahoo.co.in

[2]*Department of ECE*
Vel Tech Rangarajan Dr.Sagunthala R&D Institute of Science and Technology,
Avadi, *Chennai.*

Abstract: Blindness is a growing problem worldwide. The major causes of blindness are glaucoma and diabetic retinopathy. Increased intraocular pressure causes glaucoma. In glaucoma detection, it is very difficult to identify the edge of the optic cup because the image is blurred where blood vessels pass through the optic cup. Current methods do not effectively address the issue of peripheral blurring of the blood vessels surrounding the optic cup. In this paper, it is recommended to automatically detect glaucoma in retinal images using an efficient method. Initially, optic disk and cup segmentation is done by the Convolution Neural Network (CNN) and Modified Region Growing Mechanism (MRG). Then, texture features are extracted from the separated results. Finally, a neural network is used to diagnose glaucoma. The experimental results demonstrate that the proposed approach achieves better glaucoma detection result (accuracy, sensitivity and specificity) compared to few other approaches.

Keywords: Glaucoma detection, convolution neural network, optic cup, optic disc, modified region growing, segmentation.

1. Introduction

Glaucoma is a disease of the optic nerve that threatens the eyesight of the patients and is one of the leading causes of blindness. If undiagnosed, glaucoma causes irreversible damage to the optic nerve leading to blindness [1]. Therefore diagnosing glaucoma at early stages is extremely important for an appropriate management of the first-line medical treatment of the disease and to stop disease progression. Accurate diagnosis of glaucoma requires three different sets of examinations: Evaluation of the intraocular pressure (IOP) using contact or noncontact tonometry also known as “air puff test” or Goldman tonometry, evaluation of the visual field and evaluation of the optic nerve head damage [2]. The optic nerve head

examination (cup-to-disc ratio) is the most valuable method for diagnosis glaucoma structurally. The optic disc is the area where the optic nerve and blood vessels enter the retina. The optic cup is the white, cup-like area in the center of the optic disc [3]. Glaucoma produces additional pathological cupping of the optic disc. As glaucoma advances, the cup enlarges until it occupies most of the disc area. The normal cup-to-disc ratio is 0.3. A large cup-to-disc ratio may imply glaucoma [4]. Retinal images can be used to extract features for glaucoma analysis. For optic disc one of the major part of retinal images. The optic disc segmentation is clearly explained in these literatures [29,30]. Similarly, blood vessel segmentation is explained in [31,32].

The feature extraction from Optic Nerve Head helps in automatic detection and it is a non-invasive technique. The difference between the normal image and the glaucoma image can be determined by the change in its texture and intensities [5]. The texture is a pattern of a particular image which changes when the structural changes happen in the diseased image. There are many texture features which can be extracted from an image to understand clearly about the disease and also the type of structural changes [6]. There are two types of features like structural features and textural features. These feature changes as the texture changes due to symptoms of glaucoma [7]. Thus by using the extracted features the change in the image texture can be detected and it is worth to classify the images into two different classes such as normal and glaucomatous [8]. Due to the glaucoma disease, the structure of an image changes which results in texture and intensity changes. Hence the feature of glaucoma image differs from that of the normal image. These features are extracted and segmented for affected regions. Here, the optic disc and optic cup are segmented using the extracted features [9].

There are clinical methods available for detection of glaucoma such as tonometers (measures IOP), optical coherence tomography (OCT) (generates 3D image of the eye tissue), scanning laser ophthalmoscope (SLO) (provides 2D scan of the optic cup), and scanning laser polarimeter (SLP) (gives information about the degradation of retinal nerve fiber (RNF)) [10]. These methods are expensive, manual, time-consuming and require skilled supervision [11]. There are a few ways to deal with the advancement of PC vision algorithms for glaucoma detection based on eye fundus pictures. The first approach is to decide the nearness of the illness specifically from fundus pictures, which includes either manual or automatic extraction of picture features, got from shading, position and pairwise connection of pixels. Another approach is to assemble the algorithm for optic disc and cup segmentation, then, based on that, read out disc and cup dimension and from that judge on the presence of the disease [12]. The main contribution of the proposed method is,

- To segment the optic disc using Convolution Neural Network
- To segment the optic cup from optic disc using Modified Region Growing algorithm
- To detect the glaucoma, neural network structure is used here.

The rest of the paper is organized as follows: Section 2 provides an overview of related tasks in the field. Section 3 describes the proposed model that has different phases of the proposed task. Section 4 reveals the test results and discussion and section 5 presented conclusion of the research.

2. Related Works

A lot of researchers have experimented optic disc and optic cup based glaucoma detection in retinal images. Among them some of the works are analyzed here; Jun Cheng *et al.* [13] has presented super-pixel classification based optic cup segmentation for glaucoma detection. In optic disc segmentation, histograms, and center surround statistics were used to classify each superpixel as disc or non-disc. A self-assessment reliability score was computed to evaluate the quality of the automated optic disc segmentation. For optic cup segmentation, histograms and center surround statistics, the location information was also included in the feature space to boost the performance. but this method was given the poor segmentation results.

Moreover, Gopal Datt Joshi *et al.* [14] has exhibited OD and OC Segmentation from monocular colour retinal images for glaucoma assessment. They introduced a OD segmentation method which integrates the local image information around each point of interest in multi-dentinal feature space. For cup segmentation, they used anatomical evidence such as vessel bends at the cup boundary. The method was evaluated on 138 images comprising 33 normal and 105 glaucomatous images against three glaucoma experts. Even though, in some cases the method was produced irregular OD shapes.

In [15], Pardha Saradhi Mittapalli and Giri Babu Kande have presented a glaucoma expert system based on the segmentation of OD and optic cup attained from color fundus images. Here, implicit region based active contour model was utilized for OD segmentation and structural and gray level properties of cup utilized for OC segmentation. Based on the precise information about the contours of OD and cup different parameters were calculated for glaucoma assessment. Here, some patients have small CDR but significant visual field loss, whereas some have large CDR with little visual field loss.

Similarly, Suman Sedai et al. [16] have presented a fully automatic regression-based method which accurately segments optic cup and disc in retinal color fundus image. A data augmentation approach was developed to improve the regressors' performance by generating synthetic training data. In [17], Artem Sevastopolsky et.al, have experimented glaucoma detection based on deep learning, namely, modification of U-Net convolutional neural network.

Moreover, Muhammad Nauman Zahoor *et al.* [18] have presented a hierarchical technique for fast and accurate Optic Disc localization and segmentation. Retinal vasculature and pathologies were delineated and removed by using morphological operations at preprocessing stage followed by circular Hough transform for optic disc localization. The precise boundary of optic disk was obtained by calculating the region of interest and applying a polar transform based adaptive thresholding.

Similarly, Julian Zilly *et al.* [19] has presented a method to segment retinal images using ensemble learning based convolutional neural network (CNN) architectures. An entropy sampling technique was used to select informative points thus reducing computational complexity while performing superior to uniform sampling. The output of the classifier was subject to an unsupervised graph cut algorithm followed by a convex hull transformation to obtain the final segmentation.

3. Proposed Glaucoma Detection Framework

The main objective of the proposed methodology is to segment the optic disc and optic cup from the retinal image using convolution neural network for glaucoma detection. Glaucoma is a chronic eye disease which handles to lasting vision loss. There are different methods applied to inquire glaucoma such as enhanced Intraocular Pressure (IOP) measurement, assessment of abnormal visual field and damaged optic nerve head assessment. Out of which optic nerve head assessment is more reliable and sensitive. Therefore, in this paper, we suggest an efficient glaucoma detection technique established on optic nerve head assessment. The novelty of the proposed method is used to segment both optic disc and optic cup using CNN and MRG algorithm. These two segmentation leads to the accurate detection of glaucoma. The overall process of the suggested methodology is afforded in figure 1.

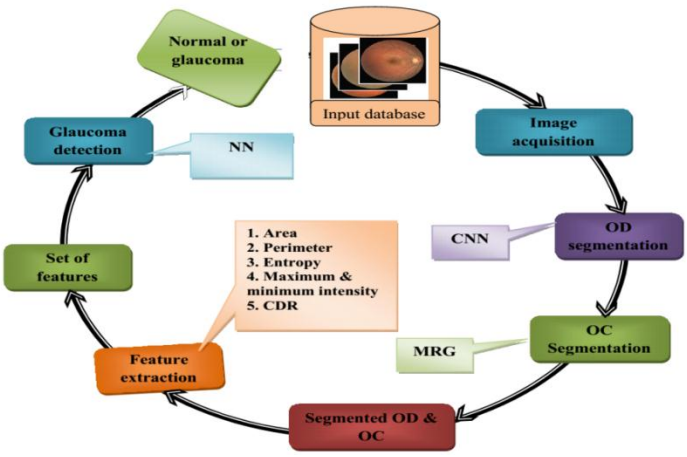

Figure 1: Overall diagram of a proposed glaucoma detection methodology

Let $D_k : k = 1,2,..., N$ be a database image. Where k is the number of images from the database and D_c is one of the images in the database D_k. In the proposed methodology implementation, initially, we perform image acquisition using an image database (D_k) of retinas. Then, we randomly select the images from the database D_k and perform CNN training process to segment the optic disc O_D from the input image D_c. After that, we segment the optic cup O_C from optic disc O_D using Modified Region Growing. Then, we extract features from segmented optic disc O_D and optic cup O_C. Finally, the extracted features are given to a softmax classifier for glaucoma detection.

3.1 Image acquisition

In this work, we utilize database created through Segmentation done by Human Experts. The images were acquired applying a Canon CR5 non-mydriatic3-CCD camera with a 45◦ field of view (FOV). Each image is captured applying 8 bits per color plane at 768 ×584 pixels. The FOV of each image is circular with a diameter of approximately 540 pixels. The some of the images are given in figure 2.

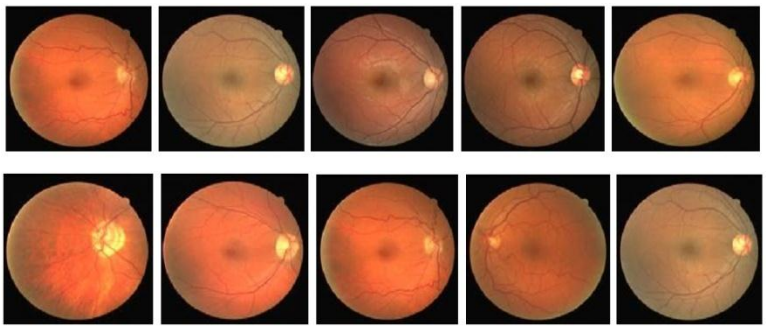

Figure 2: Illustrated the Sample images from the DRIVE database

Consider the database $D_k : k = 1,2,...,N$. The dataset consists of the different level of glaucoma. So, we divide the dataset into two groups such as $A_i : i = 1,2,...,N$ and $B_j : j = 1,2,...,N$. Where, A_i, B_j a group of images from the database D_k and i, j is the number of images from A_i and B_j. The group A_i consists of the high level of glaucoma and respective optic disc marking. The image A_c is considered as the retinal image taken as the database A_i. Similarly, the group B_j consists of normal retinal images with respective optic disc marking. The image B_c is considered as the retinal image taken as the database B_j. The collected images are given as the further processing.

3.2 Optic disc segmentation

After the image acquisition, we randomly select images from A_i and B_j. Then, the selected images are given to the CNN to segment the optic disc O_D. In CNN training, the retinal image and the corresponding OD marked image are considered as the input.

Convolution neural network architecture

CNN is a neural network established on deep learning (DL) and is a variation of the multilayer perceptron (MLP). CNN is established on the processing of visual information by using filters to the information and safeguarding relationships among the neighboring image pixels within the convolution network [20]. The convolution is a specialized type of linear operation and treats a matrix with a kernel. Figure 3 shows an example of a convolution. Figure 3(a) shows the matrix of the image to be filtered, Figure 3(b) shows the filter or kernel, and Figure 3(c) shows the convolution result.

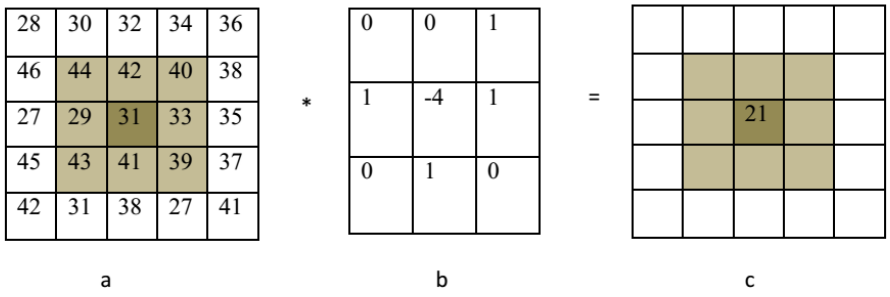

Figure 3: Convolution process (a) input image matrix (b) filter or kernel and (c) convolution result

Convolution operation performs dot products among the filter and local regions of the input. Figure 3 explains the numerical example of a simple convolution process. Here, the filter in figure 3(b) reads all the pixels in the input in figure 3(a). After this calculation, pixel 31 of the array in figure 3(a) gets 21 which are afforded in resulting matrix in figure 3(c). The calculation is:

$(44*0)+(42*1)+(40*0)+(29*1)+(31*-4)+(33*1)+ (43*0)+(41*1)+(39*0)=21.$

The most famous layers in the CNN are convolution layers and pooling layers. The convolution layer consists of a rectangular matrix of neurons. It just plays a convolution on the information of the past layer, where the weights specify the convolution filter. In CNN, each layer comprises a number of nodes, organized into maps that are combined to nodes in the next layer. Layers are composed of three main types such as convolution, max-pooling and fully-connected. The parameter of a simple convolution neural network is explained below;

Input layer: - The input image [32x32x3] comprises of pixels of the image. For example, we conceive the image of width 32, height 32 and with three color channels R, G, B.

Convolution layer: - Convolution layer is utilized to equate the yield of neurons that are associated to local regions in the input, each calculating a dot product between their weights and a little region they are combined to in the input volume. This may result in volume such as [32x32x12] if we decided to use 12 filters.

Rectified-linear non-linearity (ReLU) layer: - This layer is utilized for calculating element-wise activation function, such as the max (0,x) thresholding at zero. This leaves the size of the volume unchanged ([32x32x12]).

Pooling layer: - Pooling layer is used to perform down sampling operation, resulting it produce a volume of size [16x16x12].

Fully-connected layer: - This layer is utilized to compute the class scores, will compute the class scores, resulting in a volume of size [1x1x10], and where 10 represent the class score. In this way, ConvNets transform the original image layer by layer from the original pixel values to the final class scores.

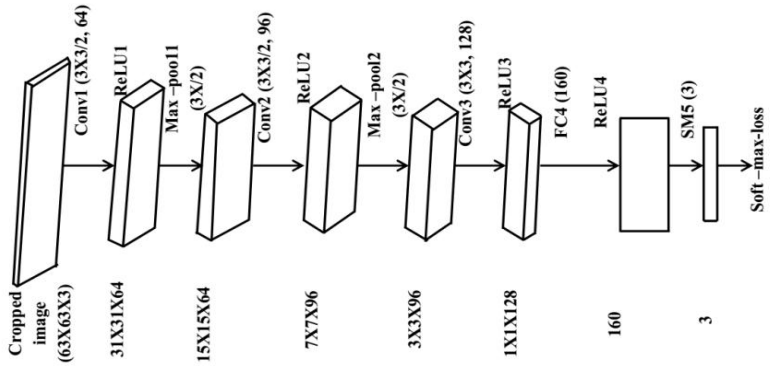

Figure 4: CNN architecture for OD segmentation

In this proposed methodology, CNN architecture is used to segment the OD in retinal image present in the database D_k. For glaucoma detection, the OD region must be separate from the input retinal image D_c. The convolution network architecture, which has accomplished great outcomes in the quick and exact segmentation of medical images, therefore, in his paper we utilized CNN for OD segmentation. Figure 4 establishes the architecture and layers of CNN. The proposed CNN consists of two paths such as contraction path and expansive path. The contraction path is given in the left side and expansive path, which is given in the right side. The contraction layer comprises of the repeated use of two 3x3 convolutions, each followed by ReLU activation function and a 2x2 max-pooling operation with stride-2 for down sampling, minimizing the width and height of the image by two. Each layer working description is already explained in this section. The x-y size is afforded in the lower left margin of the rectangle. Each progression in the expansive path consists of an up sampling of the feature map define by a 2x2 convolution ("up-convolution"), a concatenation with the correspondingly cropped feature map from the contracting path, and two 3x3 convolutions, each taken after by a ReLU. The cropping is crucial because of the loss of edge pixels in each convolution. At the last layer, a 1x1 convolution is applied to map 64- component feature vector to the coveted number of classes. Altogether the system has 23 convolution layers.

Training

After the CNN architecture design, the next step is to select the input images to the train the network. For this reason, we split the dataset D_k into two sets such as training and testing. Already, the data set has two groups $A_i : i = 1,2,..,N \; and \; B_j : j = 1,2,...,N$, among them, we randomly select 80% of images for training T_R and remaining 20% of images are selected as testing T_V. Now, T_R and T_V has a combination of $A_i \; and \; B_j$ group images. For CNN training, in this work, the input image and their corresponding segmentation maps (which derive from a specialist) are used to train the network. In CNN, each map indicates the corresponding output of the network. That is, in the learning procedure, we anticipate that CNN to learn to perceive the properties of the OD and restore a picture that comprises the segmentation of the OD region. The convolution filter weights are arbitrarily aligned at the beginning of every training process to avoid any learning interference among the experiments

in the training process. After this training process, we analyze the images by applying CNN architecture. The segmentation output is afforded in figure 5.

Figure 5: Segmentation output (a) input image and (b) segmented output image

3.3 Optic cup segmentation

After OD segmentation, we have separate optic cup (OC) region from OD. For OC segmentation, in this paper, we utilize a modified region growing algorithm (MRG). Region growing method is a popular technique for image segmentation which admits seed point selection. The neighboring pixels are equated with the primary seed points to check established on some conditions, in the segmentation process, whether the neighboring pixels can add to the region or not. In the segmentation, the Seed point selection is an important task. But, this usual Region Growing method chooses the seed points by setting the intensity threshold, which has drawbacks of noise or variation in intensity that handles to over-segmentation or holes. Moreover, in this method, the shadings of real images may not be differentiated. We align the Region growing method by conceiving intensity and orientation thresholds from the pre-processed images to employ those features in the selection of seed points to discover these difficulties. The MRG based OC segmentation is explained below;

For segmenting optic cup from optic disc using MRG, at first we calculate the gradient of the image for both X-axes (O_x) and y-axis (O_y). Then, we combine (O_x) and (O_y) for gradient vector GV using equation (1)

$$GV = \frac{1}{1 + \left(O_x^{\,2} + O_y^{\,2}\right)} \qquad (1)$$

From the gradient vector, we calculate the values of orientation. Then, we segment the images into grids G_i. After that, we set two types of threshold such as intensity threshold $\left(\text{int}_{(t)}\right)$ and orientation threshold $\left(orient_{(t)}\right)$. Then, For every grid G_i, continue the following processes in step 1 until the number of grids reached a total number of grids for an image.

Step 1(a): Calculate the histogram H of each pixel in G_i.

Step 1(b): Among them, we find out the most frequent histogram of the $G_i^{\,\text{th}}$ grid and denote it as $Frequent_{(h)}$.

Step 1(c): Prefer any pixel, according to $Frequent_{(h)}$ and assign that pixel as seed point which has the intensity $\left(\text{int}_p\right)$ and Orientation $\left(orient_p\right)$.

Step 1(d): Consider the neighboring pixel having the intensity $\left(\text{int}_n\right)$ and orientation $\left(orient_n\right)$.

Step 1(e): Find the intensity and orientation difference of those pixels p and n.

(i.e.) $$D_{\text{int}} = \left\| \text{int}_p - \text{int}_n \right\| \quad (2)$$

and $$D_{orient} = \left\| orient_p - orient_n \right\| \quad (3)$$

Step 1(f): If $D_{\text{int}} \le \text{int}_{(t)}$ && $D_{orient} \le orient_t$, then add the corresponding pixel to the region and the region

is grown, else move to step 7(h).

Step 1(g): Check whether all pixels are added to the region. If true go to step 6 otherwise go to step 1(h).

Step 1(h): Re-estimate the region and find the new seed points and do the process from step 1(a).

Step 8: Stop the whole process.

Using this Modified Region Growing process, optic cup (OC) are segmented from the OD image.

3.4 Feature extraction

Once the segmentation process is over, the feature extraction process is carried out. In this paper, from the optical disk, we extract area, perimeter, entropy, maximum intensity, minimum intensity and Cup-to-Disc Ratio (CDR). Similarly, optic cup also we extract same features.

Area: The total number of pixels that lie in the corresponding segment is called as area. If we calculate the area for optic disc means, we choose an OD image and if we calculate the area for optic cup means, we select only OC image. For example $A_1, A_2, ...A_N, ...A_M$ be the concerned segment of which first N is the in the boundary region of the segment, then area=M.

Perimeter: number of pixels in the boundary of the segment area is called as Perimeter of the segment. For example $A_1, A_2, ...A_N, ...A_M$ be the concerned segment of which first N is the in the boundary region of the segment, then perimeter=N.

Entropy: The entropy or average information of an image is a measure of the degree of randomness in the image.

$$E = -\sum_i P_i \log_2 P_i \quad (4)$$

Where, P_i is the probability that the difference between 2 adjacent pixels is equal to i, and Log_2 is the base 2 logarithms.

Maximum and minimum intensity: Maximum intensity is the maximum intensity of the segment and minimum intensity is the minimum intensity of the segment. For example $I_1, I_2, ..., I_N$ be the intensity of the pixel, then $Maximum\ \text{int}ensity = Maximum(I_1, I_2, ..., I_N)$ and $Minimum\ \text{int}ensity = Minimum(I_1, I_2, ..., I_N)$.

Cup-to-Disc Ratio (CDR): Cup to disc ratio is a significant parameter indicating the expansion of the cup region. The CDR is calculated using equation 5.

$$CDR = Diameter\ of\ cup \Big/ Diameter\ of\ disc \quad (5)$$

3.4 Glaucoma detection using ANN

Once segmentation is carried out and features are extracted. Glaucoma detection is made with the help of an artificial neural network (ANN) with the Levenberg-Marquardt algorithm (LMA). LMA has a main advantage over Back Propagation algorithm (BPA) in terms of optimization of NN among the learning stage which is exceptionally needed for any approach to get a valuable algorithm. The NN comprises of three layers such as an input layer, a hidden layer and the output layer in normal [3]. The input of NN is the feature vector we have extracted from OD and OC. We split the dataset into two types such as training and analyzing for classification. The network is trained under a large set of various retinal images in order to enable them to effectively detect the presence of diabetic in a person in the analyzing phase.

Training phase: The input image is feature extracted and this feature vector is afforded as the input to the neural network in the training phase. We align afforded random weights to the node at primarily. Then, the output found from the NN is equated to the original and error is computed. Then, weights are varied applying LMA so as to minimize the error. This process is carried out for a large number of images so as to yield a stable system having weights aligned in the nodes. The retinal images of both the normal person as well as a diabetic person are afforded as input by this phase.

Testing phase: The input image is fed to the trained neural network having particular weights in the nodes and the output is computed so as to find if the person is diabetic or not in the analyzing phase.

4. Result and Discussion

The novel glaucoma detection based on convolution neural network (CNN) is performed in the working platform of MATLAB. The system is executed in a windows machine containing configurations Intel (R) Core i5 processor, 3.20 GHz, 4 GB RAM, and the operating system platform is Microsoft Window7 Professional. In the innovative technique, at first the optic disc (OD) is segmented using CNN and from OD, the optic cup (OC) is segmented using a modified region growing algorithm (MRG). Then, the features are extracted and extracted features are given to NN, to classify the image is normal or abnormal. In the new approach, several retinal images gathered from the DRIVE database (database created through Segmentation done by Human Experts) are effectively employed.

4.1 Evaluation metric

The evaluation of the proposed glaucoma detection system is carried out using the following metrics as suggested by equations, given below:

Accuracy: Accuracy is defined as the proportion between the quantity of effectively classified cases and the total effect of cases.

$$Accuracy = \frac{TP + TN}{TP + TN + FP + FN} \quad (6)$$

Sensitivity: The measure of the sensitivity is the proportion of true positives (TP) which are properly recognized. It relates to the capacity of the test to recognize positive results. The higher the sensitivity value is, the greater the likelihood of a correct diagnosis.

$$Sensitivity = \frac{TP}{FP + FN} \quad (7)$$

Specificity: The measure of the specificity is the proportion of negatives which are properly recognized. It relates to the capacity of the test to recognize negative results.

$$Specificit\,y = \frac{TN}{TN + FP} \quad (8)$$

Jaccard coefficient: The Jaccard coefficient measures similarity between finite sample sets, and is defined as the size of the intersection divided by the size of the union of the sample sets.

$$J(S_1, S_2) = \frac{|S_1 \cap S_2|}{|S_1 \cup S_2|} = \frac{|S_1 \cap S_2|}{|S_1| + |S_2| - |S_1 \cap S_2|} \quad (20)$$

Where; S_1 is the segmented region and S_2 is the ground truth. If $S_1 and\ S_2$ are both empty $J(S_1, S_2) = 1$

Otherwise $0 \le J(S_1, S_2) \le 1$

Dice's coefficient: The Dice score is regularly used to evaluate the execution of image segmentation techniques. Then the comment on some ground truth area in image and after that makes a computerized algorithm to do it.

$$D(S_1, S_2) = \frac{2|S_1 \cap S_2|}{|S_1| + |S_2|} \quad (21)$$

4.2 Experimental result

In this section, we analyze experimental results of the proposed glaucoma detection methodology. Here, OD segmentation we used CNN, OC segmentation we used MRG and glaucoma detection we used NN. The mentioned three stages results are evaluated. The visual representation of the segmentation stage is given in figure 6 and border of the segmentation image is given in figure 7.

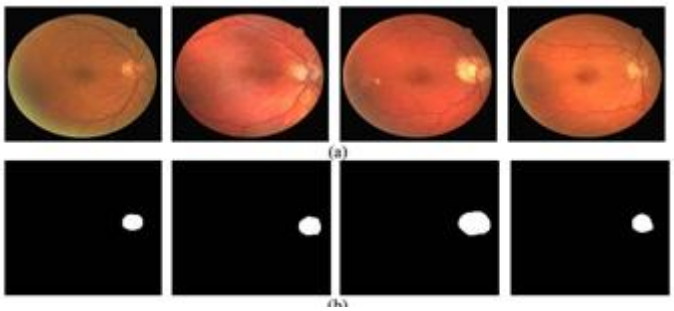

Figure 6: Experimental results of segmnetation stage (a) input image, (b) OD segmnetation result and

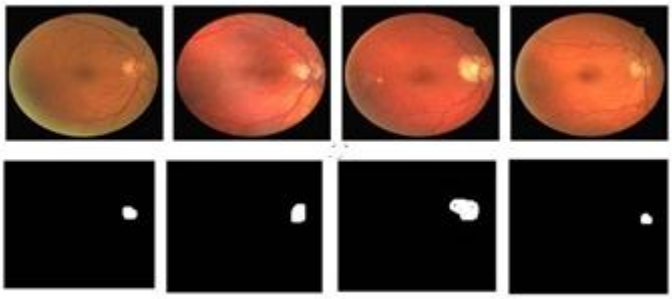

Figure 7: Optic cup segmnetation result

Table1:

Comparative analysis of proposed against existing for OD segmentation

Measures	CNN	FCM	K-means
Accuracy	94.8	90.54	87.32
Sensitivity	97.6	92.62	90.42
Specificity	96.34	93.56	91.54
Jaccard coefficient	97.57	94.32	92.43
Dice's coefficient	4.73	3.56	3.12

Table 1 contains the comparative analysis of segmentation result using proposed and existing techniques. The proposed CNN is compared with existing FCM and K-means techniques. The accuracy value obtained for existing FCM technique is 90.54 then for K-means 87.32 and finally, for the proposed CNN technique, the accuracy value is 94.8. For sensitivity, FCM occurs 92.62 then k-means obtain 90.42 and for CNN the sensitivity value is 97.6. Specificity value obtained for FCM is 93.56 then for k-means the value is 91.54 and for proposed CNN technique the sensitivity value obtained is 96.34. Similarly, our proposed method attains the maximum Jaccard coefficient of 97.57 and dice's coefficient of 4.73.

Finally, while comparing the result; our proposed CNN achieves a higher value than the existing techniques.

Table 2:

Comparative analysis of OD segmentation stage by varying iteration (accuracy)

Iteration	CNN	FCM	K-means
5	90.26	87.54	85.26
10	91.53	88.23	83.46
15	92.62	86.35	85.26
20	94.8	90.54	87.32
25	93.52	89.26	86.34

Comparative analysis for accuracy using different techniques by varying iterations is shown in table 2. The iterations were varied from 5 to 25 and the accuracy values are noted. The average value obtained for existing FCM technique is 88.384 then for k-means the average value is 85.528 and for proposed CNN the average value is 92.546. By comparing the result, our proposed CNN technique gives the better accuracy value than the existing techniques.

Table 3:

Comparative analysis of the classification stage using Accuracy measure

Iteration	ANN (%)	K-nearest neighbor (KNN)(%)	Naive bayes (%)
5	94	87	87
10	95	86	86
15	96	88	87
20	95	85	88
25	93	87	85

Table 3 shows the classification accuracy of glaucoma detection in a retinal image. The classification result is taken by varying the iterations from 5 to 25. In 5^{th} iteration, the ANN value obtained for the proposed ANN technique is 84 while KNN achieves 87% and Naive bayes gets 85%. Then for 10^{th} iteration, the proposed value obtained is 95% while KNN achieves 86% and Naive bayes achieves 84%. For 15^{th} iteration, the proposed value obtained is 96% while existing KNN gets 88% and Naive bayes gets 87%. Then for 20^{th} iteration, the proposed ANN achieves 93% while the existing KNN obtains 87% and Naive bayes gets 88%. Finally, for 25^{th} iteration, the proposed ANN value obtained is 93% while KNN gets 87% and Naive bayes achieves 85%. While comparing the result, our proposed ANN achieves maximum accuracy value. Graphical representation of table 3 is shown figure.8.

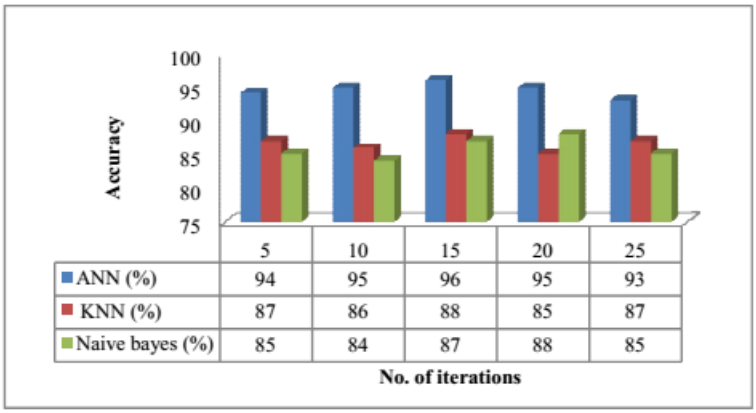

Figure 8: Graphical representation of table 3

Table 4:

Comparative analysis of classification stage using Sensitivity

Iteration	ANN (%)	K-nearest neighbor (KNN)(%)	Naive bayes (%)
5	94	87	87
10	95	86	86
15	96	88	87
20	95	85	88
25	93	87	85

Then the sensitivity value of glaucoma detection is shown in table 4. The classification result is taken by varying the iterations from 5 to 25. In a 5^{th} iteration, the ANN value obtained for the proposed ANN technique is 93 while KNN achieves 83 and Naive bayes gets 86. Then for 10^{th} iteration, the proposed value obtained is 97 while KNN achieves 87 and Naive bayes achieves 84. For 15^{th} iteration, the proposed value obtained is 95 while existing KNN gets 86 and Naive bayes gets 83. Then for 20^{th} iteration, the proposed ANN achieves 98 while the existing KNN obtains 88 and Naive bayes gets 82. Finally, for 25^{th} iteration, the proposed ANN value obtained is 96 while KNN gets 85 and Naive bayes achieves 87. While comparing the result, our proposed ANN achieves maximum accuracy value. Graphical representation of figure 9 is shown below.

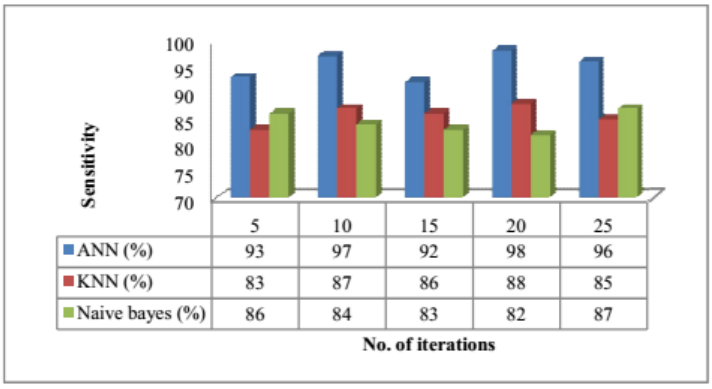

Figure 9: Graphical representation of table 4

Table 5:

Comparative analysis of classification stage using Specificity

Iteration	ANN (%)	K-nearest neighbor (KNN)(%)	Naive bayes (%)
5	94	87	87
10	95	86	86
15	96	88	87
20	95	85	88
25	93	87	85

Table 5 shows the comparative result of specificity in glaucoma detection. The proposed ANN gives the average value of 95.8% while existing KNN gets 87.2% and Naive bayes obtains 84.2%. Here the maximum value obtained is 98 during 25th iteration and the minimum value obtained is 93 for 10th iteration. Therefore, our proposed ANN gives the better performance than the existing techniques. The graphical representation of table 3 is given in figure 10.

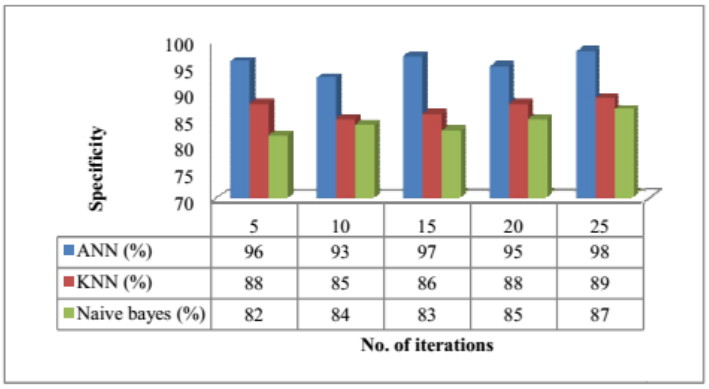

Figure 10: Graphical representation of table 4

In order to prove the efficiency of the proposed method various research papers are compared. The results are plotted in beneath,

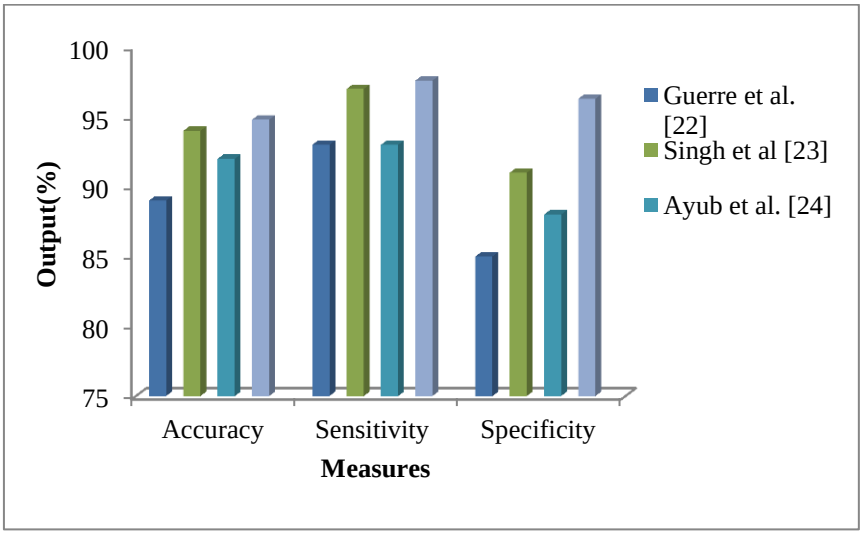

Figure 11: Comparison result of proposed and state of art methods

From the above statistics, it is clear that the proposed method achieves better results compared to the state of art method. A 94.8% accuracy rate is achieved in all images, which is higher than the methods presented with performance rates of 89%, 94% and 92%. According to the accuracy rate and the clinical context, 95 subjects were found to be well versed in 100 subjects with our proposed glaucoma detection system. For the sensitivity metric, the proposed method is obtained by 97.6%. That means that of the 100 subjects who actually suffer from glaucoma, 98 subjects will be diagnosed as glaucomatous through the glaucoma detection System. This result strengthens the ability to effectively detect glaucoma in the iris. As for the specificity, the proposed method achieves a better rate of 96.3%, which is higher than the methods presented. Of the 100 healthy subjects, over 96 subjects are considered healthy by our glaucoma detection system. Less than 4 healthy subjects are considered to be suffering from glaucoma, which represents a false but not serious alarm. From the test results, the recommended method obtains maximum efficiency compared to the state of the art method.

5. CONCLUSION

Optic disc and optic cup based glaucoma detection using convolution neural network were proposed here. By means of MATLAB, the proposed technique was performed. The proposed glaucoma detection was developed using three main stage using the optic disc and cup segmentation, feature extraction, and classification. The performance of the proposed technique was evaluated by means of accuracy, sensitivity, and specificity. For comparison, the proposed method was considered the existing technique as fuzzy c-means clustering (FCM) and k-means clustering for optic disc segmentation and KNN, Naive bayes for classification performance. From the experimental results, the proposed CNN based optic disc segmentation attained a maximum accuracy of 94.8% but the existing method attained the minimum accuracy. Similarly, in the classification stage, our proposed NN based

glaucoma detection attained the maximum accuracy of 96% but the traditional method was attained minimum accuracy. From the result, we clearly understand our proposed system was better compared to other approaches. Although the recommended method achieves maximum performance, it has some problems, such as sensitive to noise and requires large datasets to analyze the glaucoma detection. In future research, there is ample opportunity to extend the idea of the optimal glaucoma detection method to other integrated segmentation problems.

6. REFERENCE

[1] C. Muramatsu, T. Nakagawa, A. Sawada, Y. Hatanaka, T. Hara, T. Yamamoto and H. Fujita, "Automated segmentation of optic disc region on retinal fundus photographs: Comparison of contour modeling and pixel classification methods," Comput. Methods Programs Biomed., vol. 101, pp. 23–32, 2011.

[2] Medeiros, Felipe A., Linda M. Zangwill, Christopher Bowd, Roberto M. Vessani, Remo Susanna Jr, and Robert N. Weinreb. "Evaluation of retinal nerve fiber layer, optic nerve head, and macular thickness measurements for glaucoma detection using optical coherence tomography." American journal of ophthalmology 139, no. 1: 44-55, 2005.

[3] Ojima, Tomonari, Teruyo Tanabe, Masanori Hangai, Saiyuu Yu, Shiho Morishita, and Nagahisa Yoshimura. "Measurement of retinal nerve fiber layer thickness and macular volume for glaucoma detection using optical coherence tomography." Japanese journal of ophthalmology 51, no. 3: 197-203, 2007.

[4] Dutta, Malay Kishore, Amit Kumar Mourya, Anushikha Singh, M. Parthasarathi, Radim Burget, and Kamil Riha. "Glaucoma detection by segmenting the super pixels from fundus colour retinal images." In Medical Imaging, Health and Emerging Communication Systems (MedCom), 2014 International Conference on, pp. 86-90. IEEE, 2014.

[5] Vermeer, Koen A., Frans M. Vos, Barrick Lo, Qienyuan Zhou, Hans G. Lemij, Albert M. Vossepoel, and Lucas J. Van Vliet. "Modeling of scanning laser polarimetry images of the human retina for progression detection of glaucoma." IEEE transactions on medical imaging 25, no. 5: 517-528, 2006.

[6] Rajaiah, R. Preethi, and R. John Britto. "Optic disc boundary detection and cup segmentation for prediction of glaucoma." Int J Sci Eng Technol Res (IJSETR) 3, no. 10: 2665-2672, 2011.

[7] Jiang, Zhexin, Hao Zhang, Yi Wang, and Seok-Bum Ko. "Retinal blood vessel segmentation using fully convolutional network with transfer learning." Computerized Medical Imaging and Graphics 68: 1-15, 2018.

[8] Almazroa, Ahmed, Ritambhar Burman, Kaamran Raahemifar, and Vasudevan Lakshminarayanan. "Optic disc and optic cup segmentation methodologies for glaucoma image detection: a survey." Journal of ophthalmology, 2015.

[9] Acharya, U. Rajendra, Sumeet Dua, Xian Du, and Chua Kuang Chua. "Automated diagnosis of glaucoma using texture and higher order spectra features." IEEE Transactions on information technology in biomedicine 15, no. 3: 449-455, 2011.

[10] Maheshwari, Shishir, Ram Bilas Pachori, Vivek Kanhangad, Sulatha V. Bhandary, and U. Rajendra Acharya. "Iterative variational mode decomposition based automated detection of glaucoma using fundus images." Computers in biology and medicine 88: 142-149, 2017.

[11] Lim, Teik-Cheng, Subhagata Chattopadhyay, and U. Rajendra Acharya. "A survey and comparative study on the instruments for glaucoma detection." Medical engineering & physics 34, no. 2: 129-139, 2012.

[12] Artem Sevastopolsky, "Optic Disc and Cup Segmentation Methods for Glaucoma Detection with Modification of U-Net Convolutional Neural Network", Computer Vision and Pattern Recognition, 2017

[13] Jun Cheng, Jiang Liu, Yanwu Xu, Fengshou Yin, Damon Wing Kee Wong, Ngan-Meng Tan, Dacheng Tao, Ching-Yu Cheng, Tin Aung, and Tien Yin Wong. "Superpixel classification based optic disc and optic cup segmentation for glaucoma screening", IEEE transactions on Medical Imaging 32, no. 6 (2013): 1019-1032.

[14] Gopal Datt Joshi, Jayanthi Sivaswamy, and S. R. Krishnadas, "Optic disk and cup segmentation from monocular color retinal images for glaucoma assessment", IEEE transactions on medical imaging 30, no. 6 (2011): 1192-1205.

[15] Pardha Saradhi Mittapalli and Giri Babu Kande, "Segmentation of optic disk and optic cup from digital fundus images for the assessment of glaucoma", Biomedical Signal Processing and Control 24 (2016): 34-46.

[16] Suman Sedai, Pallab K. Roy, Dwarikanath Mahapatra, and Rahil Garnavi, "Segmentation of optic disc and optic cup in retinal fundus images using shape regression", In Engineering in Medicine and Biology Society (EMBC), 2016 IEEE 38th Annual International Conference of the, pp. 3260-3264. IEEE, 2016.

[17] Artem Sevastopolsky, "Optic disc and cup segmentation methods for glaucoma detection with modification of U-Net convolutional neural network", Pattern Recognition and Image Analysis 27, no. 3 (2017): 618-624.

[18] Muhammad Nauman Zahoor and Muhammad Moazam Fraz. "Fast optic disc segmentation in retina using polar transform." IEEE Access 5 (2017): 12293-12300.

[19] Julian Zilly, Joachim M. Buhmann, and Dwarikanath Mahapatra, "Glaucoma detection using entropy sampling and ensemble learning for automatic optic cup and disc segmentation", Computerized Medical Imaging and Graphics 55 (2017): 28-41.

[20] Dimovski, "Convolutional calculus", Springer Science & Business Media, Vol.43, 2012.

[21] Artem Sevastopolsky, "Optic Disc and Cup Segmentation Methods for Glaucoma Detection with Modification of U-Net Convolutional Neural Network", Pattern Recognition and Image Analysis, pp. 1-13, 2017.

[22] Guerre, A., Martinez-del Rincon, J., Miller, P., and Azuara-Blanco, A. (2014). Automatic analysis of digital retinal images for glaucoma detection. Irish Machine Vision and Image Processing Conference.

[23] Singh, M., Singh, M., and Jiwanpreet, K. (2015a). Glaucoma screening using compensated cup-to-disk ratio value.International Journal of Computer Science & Communication, 6(2):83{91.

[24] Ayub, J., Ahmad, J., Muhammad, J., Aziz, L., Ayub, S., Akram, U., and Basit, I. (2016). Glaucoma detection through optic disc and cup segmentation using k-mean clustering. In 2016 International Conference on Computing, Electronic and Electrical Engineering (ICE Cube), pages 143-147. IEEE.

[25] Tian C., Sun G., Zhang Q., et al. Integrating Sparse and Collaborative Representation Classifications for Image Classification [J]. International Journal of Image and Graphics, 2017, 17(02):1750007.

[26] Biswas B, Sen B K. Color PET-MRI Medical Image Fusion Combining Matching Regional Spectrum in Shearlet Domain [J]. International Journal of Image and Graphics, 2019, 19(01): 1950004.

[27] Shah S K. Nonrigid Medical Image Registration Based on Curves[J]. International Journal of Image and Graphics, 2017, 17(02): 1750011.

[28] Prabhanjan S, Dinesh R. Deep Learning Approach for Devanagari Script Recognition[J]. International Journal of Image and Graphics, 2017, 17(03): 1750016.

[29] Almazroa, Ahmed, Weiwei Sun, Sami Alodhayb, Kaamran Raahemifar, and Vasudevan Lakshminarayanan. "Optic disc segmentation for glaucoma screening system using fundus images." Clinical ophthalmology (Auckland, NZ) 11 (2017).

[30] Kim, Jongwoo, Loc Tran, Emily Y. Chew, Sameer Antani, and George R. Thoma. "Optic disc segmentation in fundus images using deep learning." In Medical Imaging 2019: Imaging Informatics for Healthcare, Research, and Applications, vol. 10954, p. 109540H. International Society for Optics and Photonics, 2019

[31] Thanh, Dang NH, Dvoenko Sergey, V. B. Surya Prasath, and Nguyen Hoang Hai, "Blood vessels segmentation method for retinal fundus images based on adaptive principal curvature and image derivative operators", International Archives of the Photogrammetry, Remote Sensing & Spatial Information Sciences (2019).

[32] Aguirre-Ramos, Hugo, Juan Gabriel Avina-Cervantes, Ivan Cruz-Aceves, José Ruiz-Pinales, and Sergio Ledesma. "Blood vessel segmentation in retinal fundus images using Gabor filters, fractional derivatives, and Expectation Maximization." Applied Mathematics and Computation 339 (2018): 568-587.